



Published in final edited form as:

Biopolymers. 2004 August 15; 74(6): 467–475. doi:10.1002/bip.20098.

Ultrabright Fluorescein-Labeled Antibodies Near Silver Metallic Surfaces

Joseph R. Lakowicz, Joanna Malicka, Jun Huang, Zygmunt Gryczynski, and Ignacy Gryczynski

Center for Fluorescence Spectroscopy, University of Maryland at Baltimore, Department of Biochemistry and Molecular Biology, 725 West Lombard Street, Baltimore, MD 21201

Abstract

Fluorescein-labeled antibodies are widely used in clinical assays and fluorescence microscopy. The fluorescent signal per labeled antibody is limited by fluorescein self-quenching, which occurs when the antibody is heavily labeled with multiple fluoresceins. We examined immunoglobulin G (IgG) when labeled with 0.7 to about 30 fluoresceins per antibody molecule. The extent of self-quenching was decreased, and the signal increased, when the labeled antibody was in close proximity to metallic silver particles. Time-resolved measurements showed that the intensity increase was due in part to a silver-induced increase in the radiative decay rate. These results suggest the use of labeled antibodies conjugated to silver particles as ultrabright probes for imaging or analytical applications.

INTRODUCTION

Fluorophore-labeled antibodies are widely used in fluorescence microscopy, immunoassays, and flow cytometry.^{1–4} Fluorescein and rhodamine are perhaps the most widely used probes in these applications. Typically, one wishes to obtain the largest possible signal per labeled immunoglobulin (IgG) molecule. The obvious approach is to label the IgG molecules with multiple fluorophores. Unfortunately, this procedure often results in decreased intensities because of self-quenching between the nearby probe molecules. In fact, self-quenching of fluorophores with small Stokes' shifts, which occurs for fluorescein and rhodamine, is one of the earliest observations in fluorescence spectroscopy.^{5–7} Self-quenching is due to resonance energy transfer (RET) between the probes. In the case of fluorescein, the Forster distance for RET is about 47 Å,⁸ which would include a significant fraction of the IgG molecule.

In recent reports we described the effects of metallic silver particles on nearby fluorophores.^{9–18} These studies include the effect of fluorophore–SIFs distance on fluorescence enhancement,¹¹ and brightness enhancements on silvered surfaces such as silver island films (SIFs),^{12–15} deposited colloids,^{16,17} or fractal nanostructures.¹⁸ The magnitude of fluorescence enhancement depended not only on silvered surface but also on the number of deposited fluorophores. The fluorophore–metal interaction is strong enough to compete with external and internal deactivation of excited molecules. In the present report we describe an approach to decrease severe self-quenching of fluorescein and increase the intensity per molecule of heavily labeled antibody. In previous reports we already observed a release of self-quenching in oligonucleotide¹⁹ and human serum albumin²⁰ labeled with few fluoresceins. However, in these systems the labelings were limited to 5 and 9 dyes per molecule, respectively, and did

not include immunoreagent molecules. In the present report we found that the intensity per heavily labeled IgG molecule could be increased 40-fold when localized near the silver surface.

MATERIALS AND METHODS

Labeling of IgG

Two milligrams of human immunoglobulin G (human IgG, reagent grade; Sigma) was dissolved in 1 mL of 0.1M bicarbonate buffer (pH 9.2) and mixed with 1–120 μL of fluorescein-5-isothiocyanate (FITC; Molecular Probes) solution in DMSO (2 mg FITC/200 μL DMSO). The reaction mixture was incubated for 2 h at room temperature (or at 37°C for the highest labeling) and the labeled protein (FITC–IgG) was separated from the unreacted probe by passing over a Sephadex G-25 column equilibrated with 0.1× phosphate buffered saline (PBS).

Determining the Degree of Labeling

The ratio FITC/IgG in stock solution of labeled protein was determined by independent measurements of dye and FITC–IgG concentrations, respectively. The amount of FITC was calculated using absorbance of FITC–IgG conjugates in 0.1M bicarbonate buffer (pH 9.2) at 495 nm and molar extinction coefficient of FITC $\epsilon(495 \text{ nm}) = 76,000 \text{ M}^{-1} \text{ cm}^{-1}$. The IgG concentration was determined by using Coomassie[®] Plus Protein Assay Reagent (Pierce, IL, USA). For fluorescence measurements we used the samples with average FITC/IgG ratios of 0.7, 1.1, 3.0, 8.1, 12.7, 25.6, and 29.9.

Preparation of SIFs

SIFs on quartz slides were prepared as described previously.¹⁰ Before SIF deposition quartz slides were covered with polylysine (0.01% polylysine in 0.1× PBS buffer spin coated at 3000 rpm) and only half of each slide was coated with SIF. Such prepared quartz slides were used as cover windows in 0.5 mm demountable cuvettes.

IgG–FITC Deposition

Two hundred fifty microliters of 1 μM FITC–IgG solution in 0.1× PBS was deposited on each quartz slide (half coated with SIF), as shown in Scheme I, and placed in humid chamber at 5°C overnight. IgG binds spontaneously to the surfaces. Next, slides were washed 3 times with 0.1× PBS and covered with one part of 0.5 mm demountable cuvette filled up with 0.1× PBS.

Fluorescence Measurements

All measurements were performed using front-face geometry in a 0.5 mm path way demountable cuvettes (0.5 × 12.7 × 45 mm). As described above, one half of the cover slide of the cuvette was coated with SIFs (S) and another half was unsilvered (Q) (Scheme I).

Emission spectra were collected on SLM 8000 spectrofluorometer with excitation 488 nm from a Xenon lamp. Lifetimes were measured on 10-GHz frequency-domain fluorometer using mode-locked argon ion laser 514 nm, 76 MHz repetition time. Excitation and emission polarizers were in the magic angle orientation, that is, the excitation polarizer was vertical in the lab axis and the emission polarizer 54.7° from the vertical. Emission was collected with combination of 514 nm SuperNotch plus filter (Kaiser Optics) and 540 nm interference filter. The background from unlabeled IgG coated SIF was less than 1% for all FITC–IgG samples. The background on quartz was less than 2%, for FITC–IgG with lower labeling and about 5% for highly labeled FITC–IgG.

The frequency domain (FD) intensity decay were analyzed in terms of the multiexponential model

$$I(t) = \sum_i \alpha_i \exp(-t/\tau_i) \quad (1)$$

where the τ_i 's are the lifetimes with amplitudes α_i and $\sum \alpha_i = 1.0$. Fitting to the multiexponential model was performed as described previously.^{21,22} For a single fluorophore that displays a multiexponential decay, the values of α_i represent the molecular fractions of each component. However, due to the altered rates of radiative decay, the values of α_i in the presence of silver particles are no longer the molecular fractions. The contribution of each component to the steady state intensity is given by

$$f_i = \frac{\alpha_i \tau_i}{\sum_j \alpha_j \tau_j} \quad (2)$$

where the sum in the denominator is over all the decay times and amplitudes. The mean decay time is given by

$$\bar{\tau} = \sum_i f_i \tau_i \quad (3)$$

The amplitude-weighted lifetime is given by

$$\langle \tau \rangle = \sum_i \alpha_i \tau_i \quad (4)$$

For the purpose of adjusting the amplitudes of an intensity decay, we use $\langle \tau \rangle$ because prior to normalization of $\sum \alpha_i$, the value of $\langle \tau \rangle$ represents the area under the decay and the steady state intensity.

RESULTS

Fluorescence Spectra Properties of FITC-IgG in Solution

Prior to describing the effects of SIFs, it is informative to describe the spectral properties of FITC-IgG. Figure 1 shows the emission spectra of FITC-IgG with molar labeling rates of 0.7–25.6. The emission spectra remain essentially the same for all degrees of labeling. These emission spectra are adjusted to represent the intensity for the same optical density at the excitation wavelength, and thus represent the intensity per fluorescein molecule, and not the intensity per IgG molecule. This intensity progressively decreases as the labeling ratio is increased, representing a decreased quantum yield per fluorescein residue. The insert shows the steady state anisotropy, which decreases with the extent of labeling, and then increases slightly at the highest labeling ratios. A decrease in anisotropy is consistent with RET between the fluorescein residue, as has been reported previously in homogeneous solutions.^{5,6} The

increase in anisotropy (the effect known also as repolarization) for higher degrees of labeling is probably due to the shortened lifetimes of these heavily labeled samples.

We also determined the effect of fluorescein self-quenching on the intensity decays of labeled IgG. Figure 2 shows the frequency-domain intensity decay of FITC–IgG for $L = 0.7$ and 25.6. For $L = 0.7$ the mean lifetime of 3.0 ns is comparable to that of fluorescein in solution, indicating there is little if any self-quenching. For the heavily labeled sample $L = 25.6$, the amplitude-weighted lifetime is dramatically decreased to 0.38 ns, as can be judged by the shift of the frequency response to higher frequencies. The mean lifetimes for these samples are 3.72 and 0.91 ns, respectively. The intensity decay parameters for a range of labeling ratios are given in Table I, showing a progressive shortening of the intensity decay with increased labeling.

Emission Spectra of FITC–IgG on SIFs

We examined the emission spectra of FITC–IgG on SIFs. The SIFs are subwavelength size particles of metal silver bound to the quartz surface. In our case the quartz surface is coated with polylysine. The particle size and shape is irregular. The topology of a typical SIF can be found in Ref. 10. Such silvered surfaces are widely used in surface-enhanced Raman spectroscopy (SERS). We compared the emission spectra of FITC–IgG when adsorbed to quartz and to SIFs (Figure 3). For all samples the intensity was higher on the SIFs than on quartz. The extent of enhancement was larger for higher degrees of labeling, as can be seen by the 40-fold enhancement for $L = 25.6$ as compared to the 10-fold enhancement for $L = 0.7$. We do not precisely know the relative amounts of FITC–IgG bound to quartz or the SIFs. In the case of serum albumin, we found roughly the same amounts of protein bound to both types of surfaces.¹¹ We believe that roughly the same amount of IgG are bound to the quartz and SIF.

It is informative to determine the intensity per labeled protein molecule, on quartz and silver, as the labeling ratio is increased. Figure 4, top, shows the relative intensities on quartz and silver for different degrees of labeling. Assuming the same amount of protein binds to the surface independent of the extent of labeling, the intensities on each surface represent the intensity per IgG molecule. In this case the intensity of FITC–IgG on quartz (\circ) can be increased by about 4-fold by increased labeling. Similarly, the intensity of FITC–IgG on a SIF also increases about 4-fold with increased labeling (\bullet), but the overall intensity is higher. Therefore it is possible to obtain an approximate 16-fold increase in signal per labeled IgG molecule on SIFs as compared to quartz (comparing \bullet and \circ).

For most applications the most important comparison is the intensity per labeled IgG on silver and quartz. In this case the ratios are as high as 40-fold (Figure 4, bottom). It is important to recognize that this value probably represents a minimum estimate of the possible enhancements. In a previous study of a cyanine–dye on a DNA oligomer, we found the maximum enhancement occurred about 90 Å from the silver surface.¹¹ While this is only an estimate of the optimal distance, the short range of the interaction (90 Å) indicates that most of the IgG molecule bound to the quartz between the islands will be too distant from the metal surface to be affected. Furthermore, it is thought that fluorophores closer than about 40 Å from the metal surface will be quenched.^{9,11} These considerations suggest the 40-fold enhancement represents an ensemble average over a population of IgG molecules in which only a minor fraction displays increased emission. Future sample preparations with defined distances from the metal may provide substantially more signal per labeled IgG molecule.

In previous reports we described one mechanism for enhanced fluorescence on metals is an increase in the rate of radiative decay.⁹ An increase in the radiative decay rate will result in increased intensity, as shown above, and the unusual effect of decreased lifetimes. We examined the intensity decays of FITC–IgG when bound to the quartz and silver surfaces (Figure 5). For lightly labeled FITC–IgG ($L = 0.7$) bound to quartz the intensity decay is slightly

shorter than in homogeneous solution, with amplitude-weighted decay time of 3.0 and 1.94, respectively (Tables I and II). A decreased lifetime on quartz as compared to solution has been observed for several fluorophores.^{10,11} When bound to silver the intensity decay of $L = 0.7$ FITC–IgG is dramatically shortened to about 0.08 ns (Figure 5 and Table III). More dramatic changes in lifetime were observed for the more heavily labeled samples, with the amplitude-weighted lifetime decreasing to 4–7 ps on the SIFs. The dramatic change in lifetime on SIFs as compared to quartz is better visualized on the time-dependent intensity decays (Figure 6), which were reconstructed from the recovered values of α_i and τ_i in Tables II and III. In order to compare the intensity decays without α_i normalization, we adjusted the ratio of the areas under the intensity decays on silver and quartz to be the same as the ratio of the steady state intensities on silver and quartz. These plots show that all the intensity decays on silver contain a rapid initial decay followed by a slower decay, which may be due to the IgG molecules bound between the silver islands and distant from the silver surfaces. If this is true, then the increased intensity on silver is due to the short decay time component in the intensity decay.

Examination of these decays also suggests that the slow components in the decays have roughly the same decay times and amplitudes. This result supports our claim that the longer components are due to molecules bound between the SIFs and that the increased steady state intensity is due to the short lifetime components in the decays.

We were surprised by the dramatic decreased in lifetime observed on the SIFs (Tables II and III), and considered other mechanisms in addition to an increased rate of radiative decay. It is known that some clusters of fluorophores can emit superfluorescence, especially with high intensity illumination.^{23–25} Superfluorescence is defined as cooperative and/or simultaneous emission of a collection of interacting dipoles. The emission begins spontaneously, is not driven by the incident light field, and is thus not stimulated emission in the classical sense. Superfluorescence is characterized by decreased lifetimes and a narrowing of the emission spectra.^{23–25} We reasoned that interactions of the fluorophores with the metallic surfaces may lower the threshold for superfluorescence. Figure 7 shows emission spectra of heavily labeled FITC–IgG when illuminated with 10-fold more and 10-fold less light than used for the other experiments described in this report. The spectra are essentially unchanged, suggesting that superfluorescence is not occurring in our experiments. At still higher illumination intensities we have observed some spectral narrowing, but further studies are needed to determine if proximity to silver surfaces can lower the threshold for superfluorescence.

Another possible origin of the increased intensities seen on SIFs is increased rate of excitation due to an increased light field near the silver particles.^{26,27} If the rate of excitation is increased, than one expects an increased rate of photobleaching. Figure 8 shows the emission intensities of FITC–IgG on quartz and silver with continuous illumination. The relative rates are about the same. It is clear that the rate of photobleaching is not increased dramatically. Integration of the areas under the curves indicates about 13-fold more time-integrated emission can be obtained on silver as compared to quartz. This ratio is on the same order as the increased intensities on silver as compared to quartz. These results suggest that an increased rate of excitation is not the origin, or not the dominate origin, of the higher fluorescence intensities observed on SIFs.

DISCUSSION

What is the origin of fluorescence enhancement observed on SIFs? In the case of fluorophores deposited on SIFs, there are two major factors affecting the brightness of the sample. First, the enhanced local field near the islands could provide a higher excitation rate. This is somehow equivalent to the stronger excitation. Second, the radiative rate increase enhances quantum yield of fluorophores (in limit up to 1.0). This effect is responsible for decrease of lifetimes.

We believe an increased rate of radiative decay is the dominant mechanism for the increased intensities of FITC–IgG seen on SIFs. We can use the data of the relative intensities and lifetimes on quartz and silver to estimate the ensemble-averaged apparent increase in the radiative decay rate. The quantum yields (Q) and lifetimes (τ) of a FITC–IgG on quartz are given by

$$Q_q = \frac{\Gamma_q}{\Gamma_q + k_q} \quad (5)$$

$$\tau_q = \frac{1}{\Gamma_q + k_q} \quad (6)$$

where Γ is the radiative decay rate and k is the sum of the nonradiative decay rates. The radiative decay rate can be obtained from the ratio

$$Q_q / \tau_q = \Gamma_q \quad (7)$$

A similar set of equations can be written for FITC–IgG on silver, so that

$$Q_s = \frac{\Gamma_s}{\Gamma_s + k_s}, \quad \tau_s = \frac{1}{\Gamma_s + k_s}, \quad \frac{Q_s}{\tau_s} = \Gamma_s \quad (8)$$

Hence the ratio of the radiative decay rates on silver and quartz can be calculated from

$$\frac{Q_s / \tau_s}{Q_q / \tau_q} = \frac{\Gamma_s}{\Gamma_q} \quad (9)$$

where the lifetimes are then amplitude-weighted values. It is difficult to determine the quantum yields on the silver surfaces. As an approximation we assume the quantum yield on quartz is comparable to that for a FITC–IgG in solution. Given the large increases in intensity on silver, we assume all these quantum yields are unity. These calculations indicate that the apparent increase in the radiative decay rate is in the range of 30–300-fold for low and high labeling, respectively. We expect the actual increase in Γ_s / Γ_q may be larger because in our experiments, much of the FITC–IgG is probably distant from the silver surfaces.

What are the potential uses of the enhanced emission of FITC–IgG? Many immunoassays are performed with surface-bound antibodies. Hence it should be possible to obtain increased intensities on substrated coated with silver particles. This approach would also serve to provide increased signal near the bioaffinity surface and thus decrease the contribution of unwanted autofluorescence from the sample. Another possibility is to create ultrabright reagents for flow cytometry or cellular imaging. In this case the labeled antibodies would be in solution bound to silver colloids.

Acknowledgments

This work was supported by the NIH National Center for Research Resources, RR-08119, and the National Institute for Biomedical Imaging and Bioengineering EB000682.

Contract grant sponsor: NIH National Center for Research Resources (NCRR) and National Institute for Biomedical Imaging and Bioengineering (NIBIB)

Contract grant number: RR-08119 (NCRR), and EB000682, EB1690, and EB00981 (NIBIB)

References

1. Schulman, SG.; Hochhaus, G.; Karnes, HT. *Luminescence Techniques in Chemical and Biochemical Analysis*. Baeyens, WRG.; De Keukeleire, D.; Korkidis, K., editors. Marcel Dekker; New York: 1991. p. 341-380.
2. Ozinskas, A. *Topics in Fluorescence Spectroscopy, Vol. 4: Probe Design and Chemical Sensing*. Lakowicz, JR., editor. Plenum Press; New York: 1994. p. 449-496.
3. Karnes, HT.; O'Neal, JS.; Schulman, SG. *Molecular Luminescence Spectroscopy, Methods and Applications: Part 1*. Schulman, SG., editor. John Wiley & Sons; New York: 1985. p. 717-779. p. 826
4. Herzenberg LA, Parks D, Sahaf B, Perez O, Roederer M, Herzenberg LA. *Clin Chem* 2002;48(10): 1819-1827. [PubMed: 12324512]
5. Jablonski J. *Acta Phys Polon* 1955;XIV:295-307.
6. Jablonski J. *Acta Phys Polon* 1972;A41:86-90.
7. Dale RE, Bauer RK. *Acta Phys Polon* 1971;A40:853-882.
8. Kowski A. *Photochem Photobiol* 1983;38(4):487-508.
9. Lakowicz JR. *Anal Biochem* 2001;298:1-24. [PubMed: 11673890]
10. Lakowicz JR, Shen Y, D'Auria S, Malicka J, Fang J, Gryczynski Z, Gryczynski I. *Anal Biochem* 2002;301:261-277. [PubMed: 11814297]
11. Malicka J, Gryczynski I, Gryczynski Z, Lakowicz JR. *Anal Biochem* 2003;315:57-66. [PubMed: 12672412]
12. Malicka J, Gryczynski I, Maliwal BP, Fang J, Lakowicz JR. *Biopolymers (Biospectroscopy)* 2003;72:96-104. [PubMed: 12583012]
13. Lakowicz JR, Maliwal BP, Malicka J, Gryczynski Z, Gryczynski I. *J Fluoresc* 2002;12:431-437.
14. Maliwal BP, Malicka J, Gryczynski I, Gryczynski Z, Lakowicz JR. *Biopolymers (Biospectroscopy)* 2003;70:585-594. [PubMed: 14648768]
15. Lakowicz JR, Malicka J, Gryczynski I. *BioTechniques* 2003;34:62-68. [PubMed: 12545541]
16. Geddes CD, Cao H, Gryczynski I, Gryczynski Z, Fang J, Lakowicz JR. *J Phys Chem A* 2003;107:3443-3449.
17. Geddes CD, Parfenov A, Roll D, Fang J, Lakowicz JR. *Langmuir* 2003;19:6236-6241.
18. Parfenov A, Gryczynski I, Malicka J, Geddes CD, Lakowicz JR. *J Phys Chem B* 2003;107:8829-8833.
19. Malicka J, Gryczynski I, Lakowicz JR. *Anal Chem* 75:4408-4414. [PubMed: 14632044]
20. Lakowicz JR, Malicka J, D'Auria S, Gryczynski I. *Anal Biochem* 2003;320:13-20. [PubMed: 12895465]
21. Laczko G, Gryczynski I, Gryczynski Z, Wicz W, Malak H, Lakowicz JR. *Rev Sci Instrum* 1990;61:2331-2337.
22. Lakowicz JR, Laczko G, Cherek H, Gratton E, Limkeman M. *Biophys J* 1994;46:463-477. [PubMed: 6498264]
23. McGehee MD, Gupta R, Veenstra S, Miller EK, Diaz-Garcia MA, Heeger AJ. *Phys Rev B* 1998;58(11):7035-7039.
24. Frolov SV, Gellermann W, Ozaki M, Yoshino K, Vardney ZV. *Phys Rev Lett* 1997;78(4):729-732.
25. Yokoyama S, Nakahama T, Otomo A, Mashiko S. *Colloids Surfaces A* 2002;198-200:433-438.
26. Kummerlen J, Leitner A, Brunner H, Aussenegg FR, Wokaun A. *Mol Phys* 1993;80(5):1031-1046.

27. Metiu H. Prog Surface Sci 1984;17:153–320.

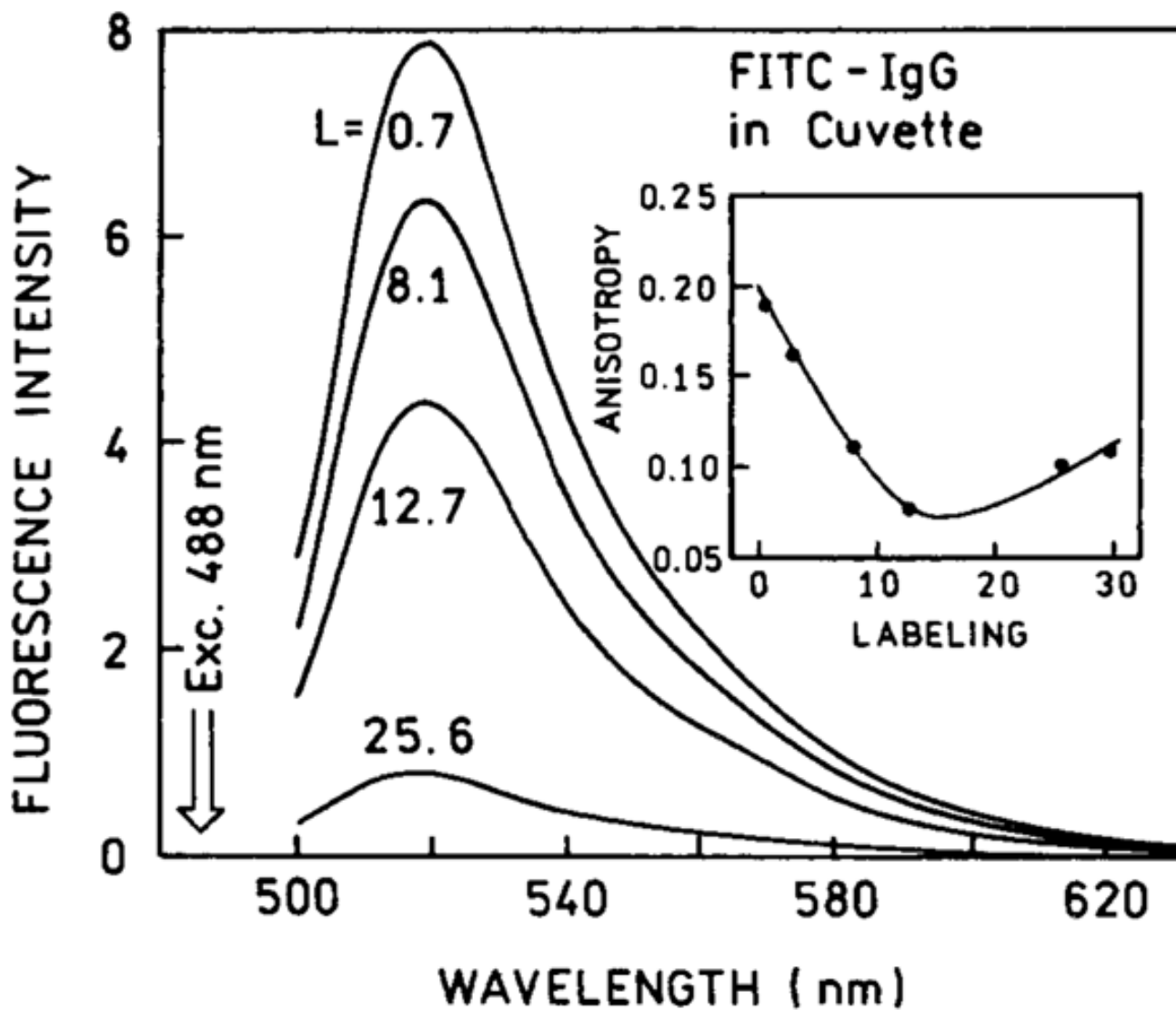


FIGURE 1.

Emission spectra of FITC-labeled IgG in the molar ratio (L) of FITC to IgG. The optical densities were matched at the excitation wavelength of 488 nm. The insert shows the steady state anisotropy for various values of L .

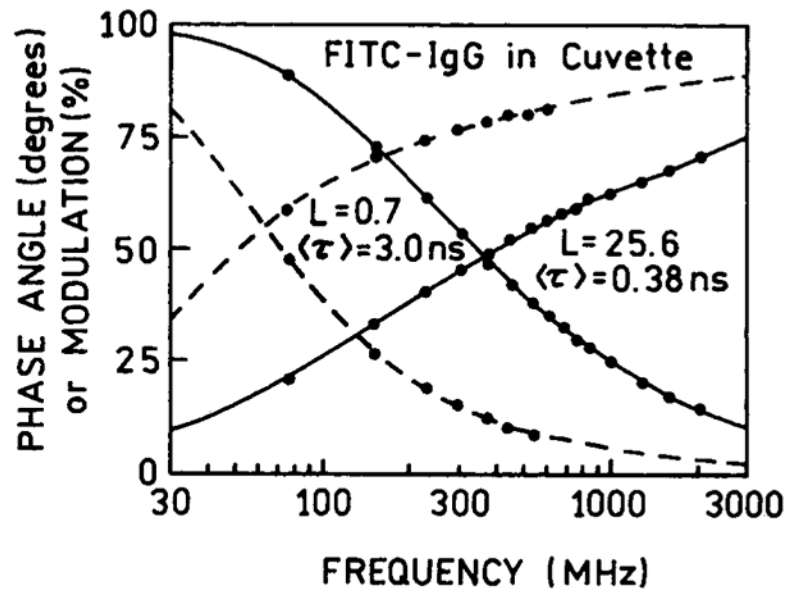


FIGURE 2. Frequency-domain intensity decay of FITC-IgG for labeling ratios (L) of 0.7 and 25.6.

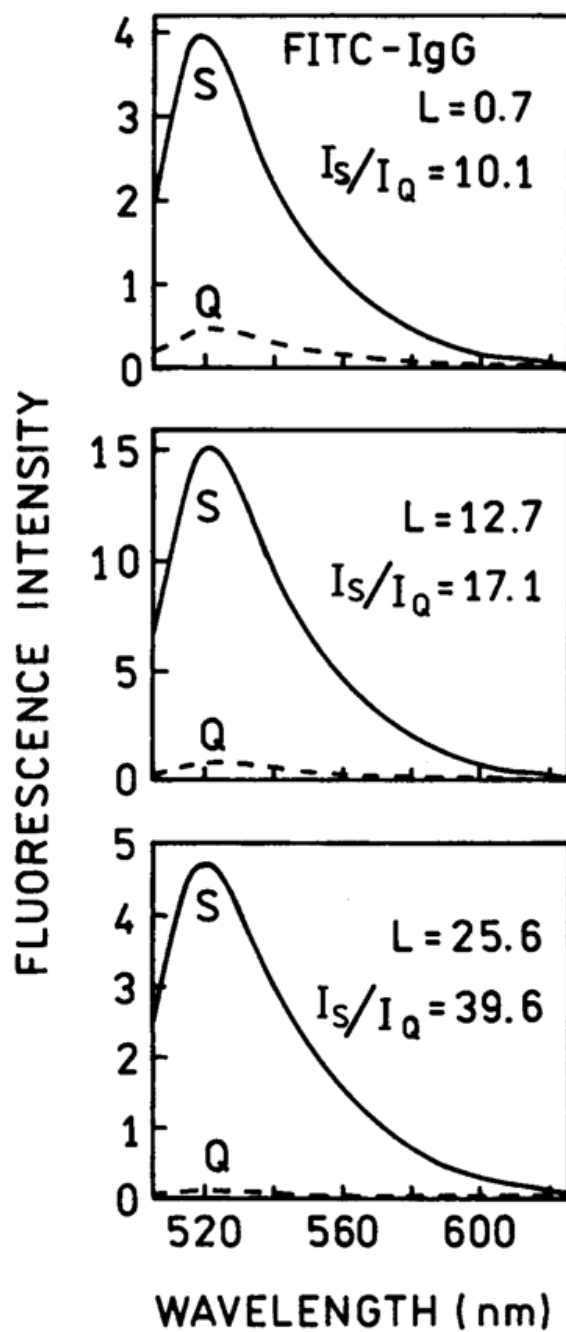


FIGURE 3. Emission spectra of FITC-IgG on quartz (- - -) and silver (—) for $L = 0.7, 12.7,$ and 25.6 . Excitation at 488 nm.

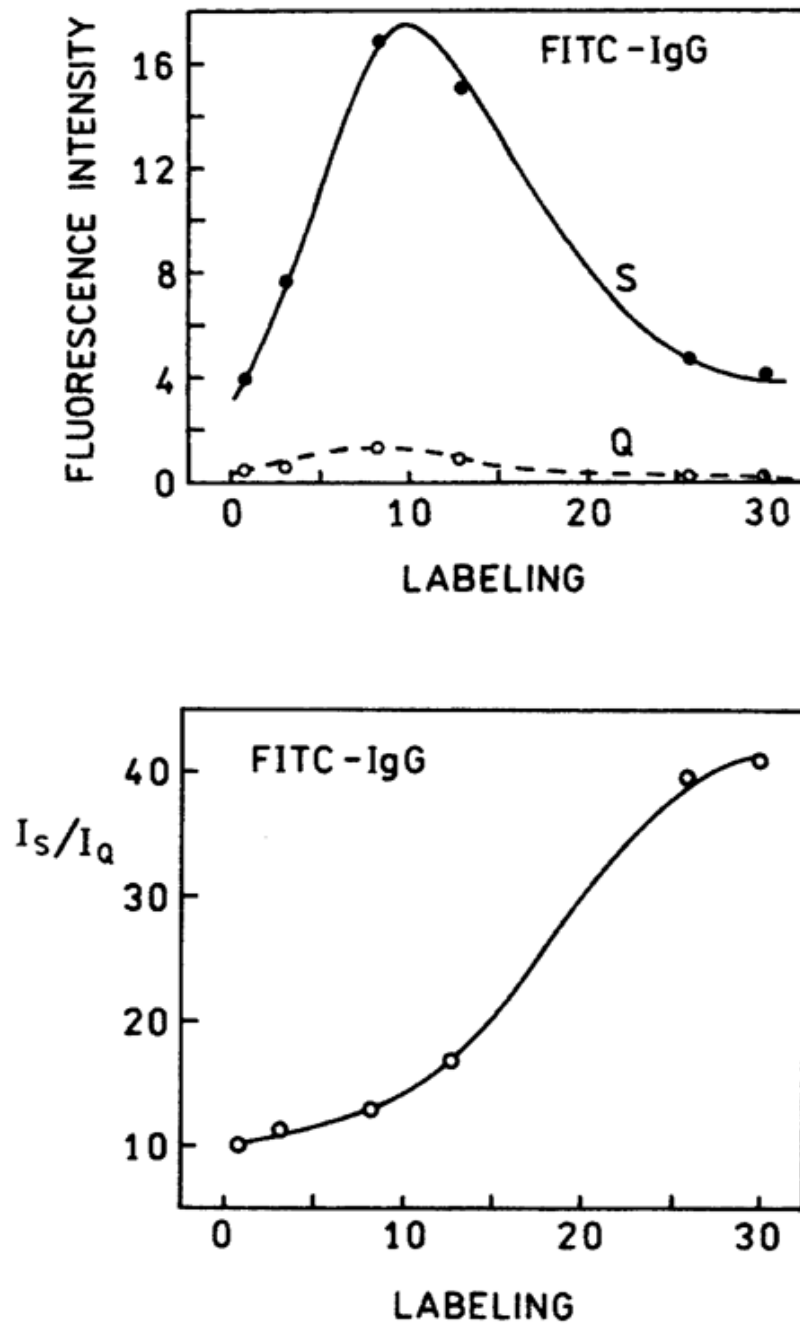


FIGURE 4. Fluorescence intensities of FITC-IgG on quartz and silver (top). Relative intensity of FITC-IgG on quartz and silver for different labeling ratios (bottom).

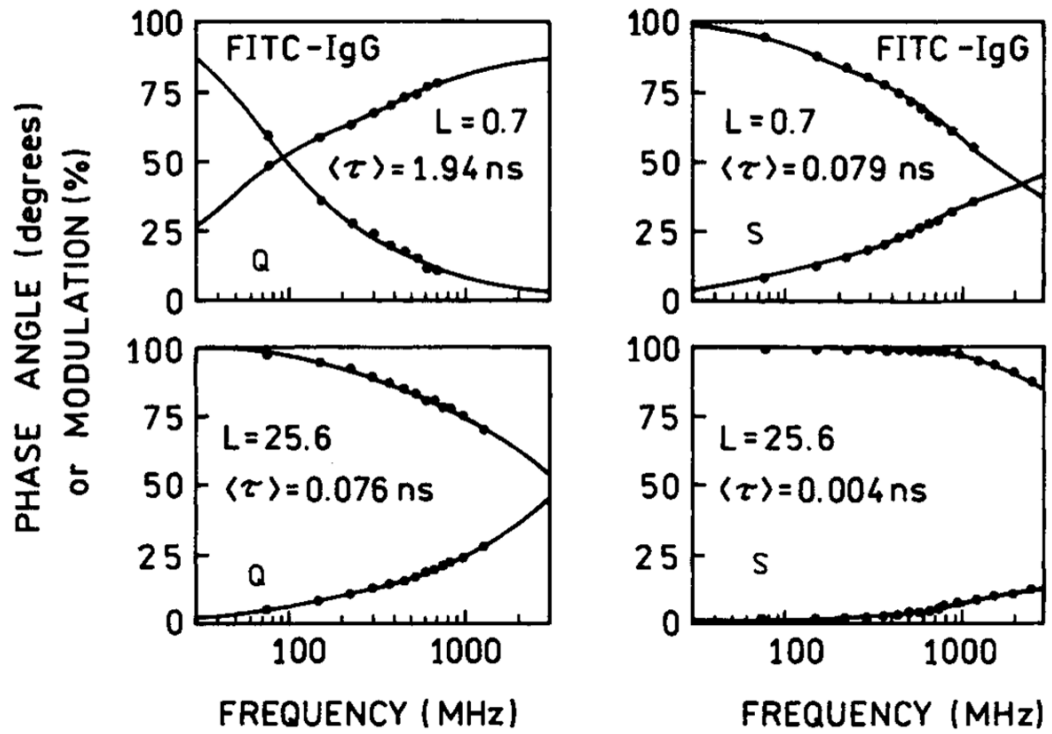


FIGURE 5. Frequency-domain intensity decays of FITC-IgG on quartz (left) and silver (right).

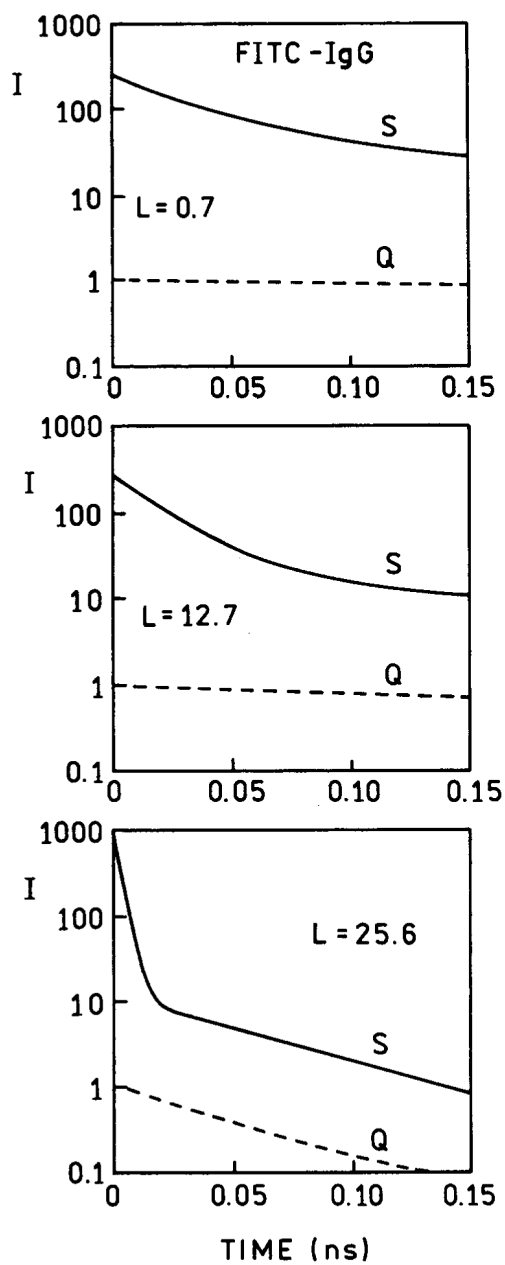


FIGURE 6. Reconstructed time-dependent intensity decays of FITC-IgG with the relative areas under the decays equal to the ratio of the steady state intensity on silver and quartz.

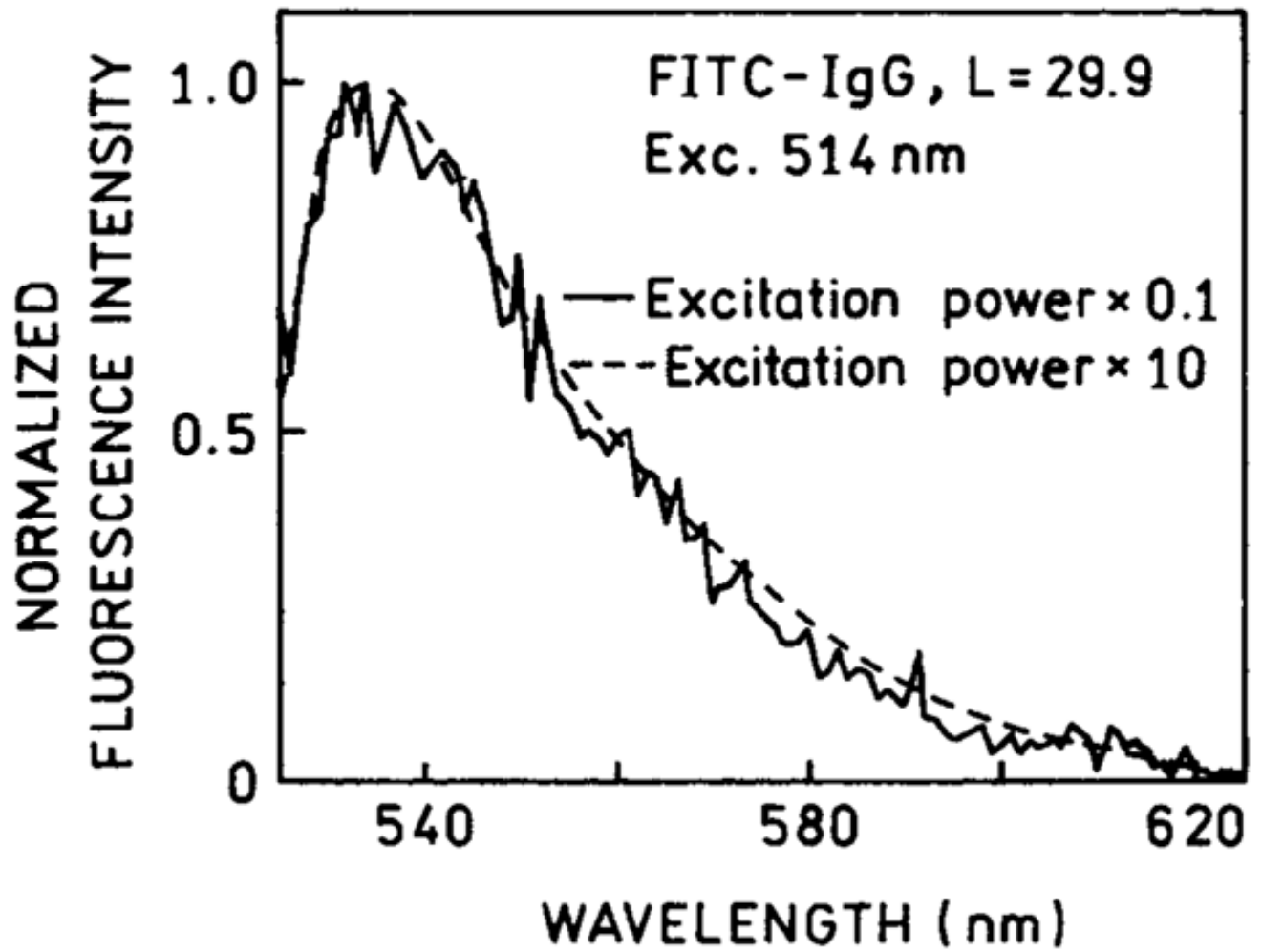


FIGURE 7.
Emission spectra of FITC-IgG ($L = 29.9$).

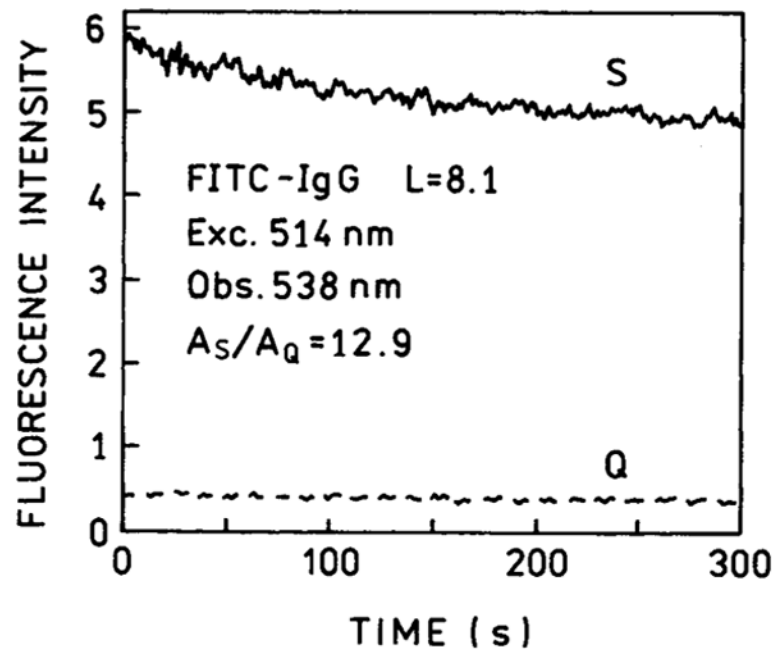
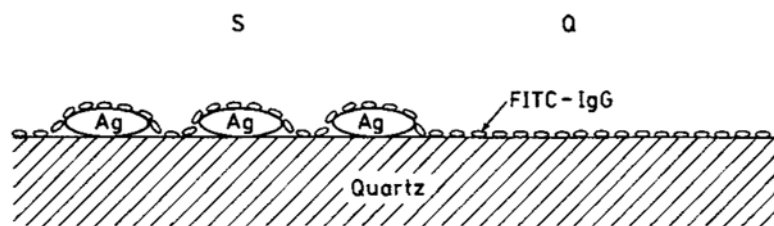


FIGURE 8. Photostability of FITC-IgG on quartz and silver. The incident intensity at 488 nm was the same for both samples.



SCHEME 1.
FITC-IgG on silver island film (S) and quartz (Q).

Table I
 Multiexponential Decay Analysis of FITC-IgG Fluorescence in Solution

<i>L</i>	Fluorescence Anisotropy	$\langle \tau \rangle$ (ns)	$\bar{\tau}$ (ns)	a_i	f_i	τ_i (ns)	χ_R^2
0.7	0.191	3.00	3.72	0.243	0.032	0.39	
1.1	0.196	2.86	3.56	0.757	0.968	3.84	0.9
3.0	0.162	2.85	3.48	0.231	0.021	0.26	
8.1	0.113	2.42	2.93	0.769	0.979	3.63	1.3
12.7	0.078	1.87	2.34	0.228	0.031	0.39	
25.6	0.103	0.438	0.908	0.772	0.969	3.58	1.6
29.9	0.109	0.382	0.889	0.231	0.035	0.37	
				0.769	0.965	3.03	1.1
				0.304	0.076	0.47	
				0.696	0.924	2.49	1.0
				0.424	0.085	0.091	
				0.406	0.393	0.440	
				0.170	0.522	1.393	0.9
				0.509	0.114	0.086	
				0.408	0.519	0.485	
				0.083	0.367	1.695	1.6

Table II
 Multiexponential Analysis of FITC-IgG Monolayer Fluorescence Intensity Decays on Quartz

L	$\langle \tau \rangle$ (ns)	$\bar{\tau}$ (ns)	a_i	f_i	$\bar{\tau}_i$ (ms)	χ^2_R
0.7	1.94	2.81	0.477	0.142	0.58	
			0.523	0.858	3.18	1.2
1.1	1.61	2.32	0.480	0.150	0.50	
			0.520	0.850	2.63	0.9
3.0	1.15	1.84	0.679	0.321	0.55	
			0.321	0.679	2.44	1.5
8.1	0.77	1.12	0.860	0.626	0.56	
			0.140	0.374	2.07	1.5
12.7	0.58	0.74	0.905	0.756	0.49	
			0.095	0.244	1.50	1.6
25.6	0.076	0.196	0.908	0.620	0.045	
			0.080	0.225	0.183	
			0.012	0.155	0.820	0.8
29.9	0.059	0.186	0.908	0.611	0.040	
			0.079	0.225	0.168	
			0.013	0.164	0.754	0.8

Table III
 Multiexponential Analysis of FITC-IgG Monolayer Fluorescence on SIFs

L	$\langle \tau \rangle$ (ns)	$\bar{\tau}$ (ns)	a_i	f_i	$\bar{\tau}_i$ (ns)	χ^2_R
0.7	0.079	0.377	0.791	0.310	0.031	
			0.197	0.482	0.194	
			0.012	0.208	1.316	1.3
1.1	0.081	0.383	0.845	0.414	0.040	
			0.142	0.367	0.213	
			0.013	0.219	1.360	2.1
3.0	0.062	0.343	0.850	0.339	0.025	
			0.137	0.432	0.198	
			0.013	0.229	1.092	1.0
8.1	0.060	0.297	0.863	0.352	0.024	
			0.125	0.454	0.214	
			0.012	0.194	0.988	0.9
12.7	0.036	0.163	0.915	0.515	0.021	
			0.083	0.421	0.187	
			0.002	0.064	1.135	1.0
25.6	0.004	0.020	0.985	0.701	0.003	
			0.015	0.299	0.059	1.1
29.9	0.007	0.025	0.980	0.789	0.006	
			0.020	0.211	0.094	0.9